Influence of Ablation on Differential Arc Resistance

Author(s):
Bort, Lorenz; Freiermuth, Vincent; Franck, Christian

Publication date:
2017

Permanent link:
https://doi.org/10.3929/ethz-b-000205908

Originally published in:
Plasma Physics and Technology Journal 4(2), https://doi.org/10.14311/ppt.2017.2.145

doi:10.14311/ppt.2017.2.145
Plasma Physics and Technology **4**(2):145–148, 2017

INFLUENCE OF ABLATION ON DIFFERENTIAL ARC RESISTANCE

L. S. J. Bort*, V. Freiermuth, C. M. Franck

High Voltage Laboratory, Eidgenössische Technische Hochschule, Zürich, Switzerland

* lbort@ethz.ch

Abstract. The influence of ablation on the du/di behavior of an arc in a model gas circuit breaker was examined. Specifically the transition from a state without ablation in the nozzle towards states with ablation was of interest, since prior work indicated that for high currents the voltage becomes constant or du/di gets even positive if ablation is present. Measurements with different blow pressures and rectangular DC currents of varying amplitude were compared, using PMMA-nozzles and dry air as blowing gas. Ablation was measured by weighing the nozzle, scanning the cross section, and using a coordinate measuring machine. The results agreed well, and confirmed that higher pressure shifts the du/di curve towards more favorable values.

Keywords: axially blown arc, ablation, passive oscillation, MRTS, HVDC CB.

1. Introduction

Unlike in AC, the interruption of DC currents requires the creation of an artificial current zero crossing. Today in DC transfer switches, such as metal return transfer switches (MRTS), the passive oscillation circuit is used. An LC-circuit is connected in parallel to a gas circuit breaker. If the arc has a negative differential resistance du/di, the damping of the oscillation in the LC-arc-loop is negative, and eventually will lead to current zero in the breaker [1]. If the arc voltage is not falling with increasing current, passive oscillation fails and additional circuitry is needed which actively brings the current to zero[2]. Previous work at HVL [3] and others [4] indicated that a high amount of ablation leads to du/di being positive, but did not analyze it in detail.

2. Setup

The setup used was previously described in [3], [5], [6]. It consists of a model gas circuit breaker, which uses gas bottles for a freely adjustable blow pressure and two contact pins of which one is movable to draw the arc. Dry air was used as a blowing gas. The inlet pressure is variable, the exhaust pressure is always fixed at 1 bar. Since no gas handling is required to access the parts, it is possible to remove and reinstall the nozzle in a matter of minutes, which made it possible to determine the ablation after each test in reasonable time.

For the measurements presented in this paper, three identical nozzles were produced. Each was used for a series of experiments of one pressure. In the following, these series are shown as 4.5 bar abs., 8.4 bar abs. and 12.7 bar abs., which refers to the inlet pressure of the nozzle. PMMA was chosen because it is transparent, making it possible to observe the arc. To allow separation along the axis of cylindrical symmetry, each nozzle consisted of two identical parts. This

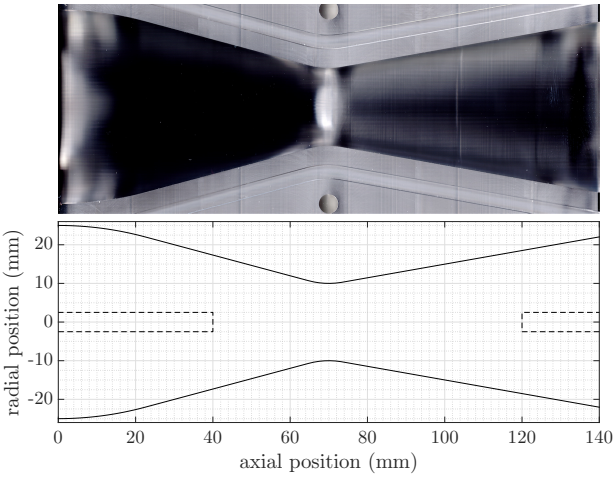

Figure 1. Top: Image of one nozzle half as captured by flatbed scanner. The contour can be seen, as well as the grooves for the sealing cord and two of the six holes for dovel pins. Bottom: Extracted nozzle contour (solid), and position of contacts (dashed). Gasflow was from left to right, cathode was left, anode right.

was achieved by milling the contour into two rectangular blocks of PMMA, which were bolted together. To ensure tightness, a rubber seal in a groove was used, and the alignment was guaranteed by dovel pins. Separating the nozzle allowed scanning the contour line in between experiments to track the changes in geometry, as described in sec. 3.

The nozzle geometry is shown in fig. 1, and identical to the one presented in [5]. The inlet directly attaches to the inlet pressure volume and has a diameter of 50 mm. Both the converging and the diverging part are conical, with half angles of 15° and 10° respectively. The throat was 70 mm after the inlet and was 20 mm in diameter initially. The contacts are copper-tungsten rods with 5 mm diameter, which were at the indicated axial positions of 40 mm and 120 mm.

3. Method

The ablation of nozzle wall material was determined using three different methods. First, the two halves where weighed with a scale, with which the mass could be determined with ±10 mg accuracy, giving ±20 mg certainty for the complete nozzle.

Secondly, the two halves were scanned with an off the shelf flatbed scanner. Assuming cylindrical symmetry, the change of the contour and the density of PMMA (1.188 mg mm^{-3}) can be used to calculate the ablated mass. Additionally, this method shows the axial location of the ablation. The scanner used had a resolution of 4800 dpi, which gives a theoretical resolution of 5 µm per pixel. The gray scale images were aligned, cropped and converted to a binary image first, and the contour of the wall was extracted afterwards using MATLAB. Figure 1 shows one example image before processing and the result.

As a third method, the inner contour of the nozzle was determined by a coordinate measurement machine (CMM) *Mitutoyo KN815*, which is usually used to compare workpieces to the specifications. This machine determined the radius every 5 mm along the axial direction, by measuring 8 points along the circumference. Since the machine was not available at the laboratory, it was only feasible to measure each nozzle before use, and two of the three after the complete series of experiments. The accuracy of these measurements was given by the roundness of the circles, which was about 20–40 µm before and 30–100 µm after all the experiments.

To create the test currents, the FPDCS current source as described in [6] was used. As shown in figure 2, each experiment consisted of two phases: During the pre-current phase, only a small current is flowing while the downstream contact moves from the closed position to the open position. This way, an arc is established. Towards the end of this phase, the current is slightly increased and the valves of the blowing system are opened. As soon as the gas flow has reached a steady state and the contact has stopped its movement at the final position, the main current phase is started. During this time, the current is increased and held at its set value for 10 ms. All results that are shown in section 4 are calculated only from the values of the main current phase.

After each measurement, the nozzle halves were weighed and the contour was scanned with the flatbed scanner, to determine the ablation. Two measurements per current setting were done to ensure repeatability, while keeping the total number of experiments - and therefore ablation - for each nozzle low, to ensure the geometry is as similar as possible for all tests. For the same reason, the measurements were done in ascending order, starting at 300 A up to 1400 A. The measurements with 100 A and 200 A however were done afterwards, when it became clear that they are desired to complete the data set. Since the ablation values of 300 A were already at the edge of the measurement range, the 100 A and 200 A tests were done with an adapted current shape. The inductance of the current source was increased, to reduce ripple and prevent the current to go to zero. Additionally the duration of the main current phase was increased from 10 ms to 40 ms, to increase the amount of ablation towards measurable values. During the complete measurement series, the throat diameter increased by a maximum of 10%, which did not change the arc voltage measurably. This was confirmed by repeating the first test at the very end.

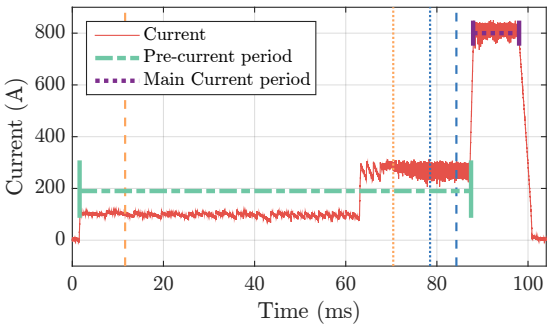

Figure 2. Example current waveform. Start and end of contact movement are indicated with vertical dashed lines, start and stabilization of blowing gas flow with vertical dotted lines. The 85 ms of pre-current were identical for all experiments, followed by 10 ms of main current, 800 A in this case.

4. Results

According to the considerations described in [5] and [7], the voltage and current data of the high current phase was evaluated using the median value instead of the mean, to be more robust against fluctuations. The error bars in figures 3 and 4 are indicating the 15.9 and 84.1 percentiles. Those percentiles give meaningful results even if the voltage fluctuations are not gaussian, and equal the standard deviation if they are. Figure 4 shows the du/di behavior is more favorable for higher blow pressures. For 4.5 bar, the voltage curve is falling up to about 400 A, and is slightly rising until it becomes flat above. For 8.4 bar the rising part is less pronounced and for 12.7 bar the rising part is not observed anymore. The curve gradually transitions into a flat regime around 800 A to 1000 A. Additionally, the overall arc voltage and arc power is higher for higher blow pressures, as shown in fig. 3.

Table 1 shows the mass that was ablated during the entire measurement series, for all three pressures. The CMM measurements agree very well with the weight measurement whereas the flatbed scanner results overestimate the mass loss by about 10%. Figure 7 shows the nozzle geometry change of the 12.4 bar series, as determined by the 29 measured circles of the CMM, and the scan. It can be seen that upstream of the throat (< 70 mm), the scan overestimates the ablation, whereas downstream it shows less in comparison with

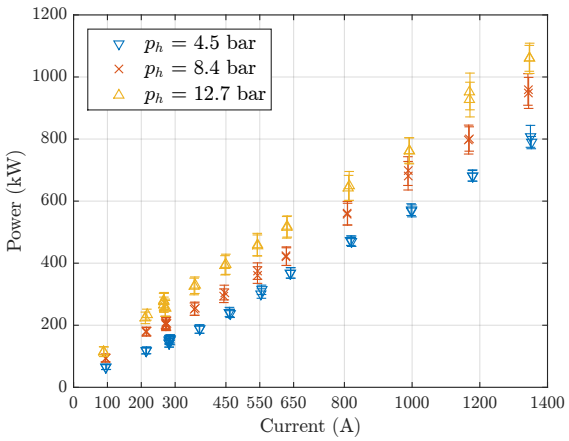

Figure 3. Arc power during the main current phase as function of current. Errorbars indicate the 15.9 and 84.1 percentiles.

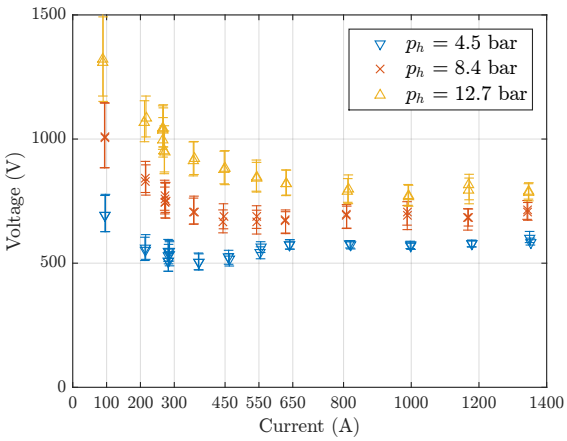

Figure 4. Arc voltage as function of current. The markers show the median, the errorbars indicate the 15.9 and 84.1 percentiles.

	Scale	Scan	CMM
4.5 bar	5.43 g	5.56 g	n/a
8.4 bar	4.05 g	4.41 g	4.14 g
12.7 bar	3.38 g	3.72 g	3.35 g

Table 1. Sum of the ablated mass of all the experiments for each nozzle, determined by weighing, the scans and the CMM. Scale inaccuracy is at least ±20 mg.

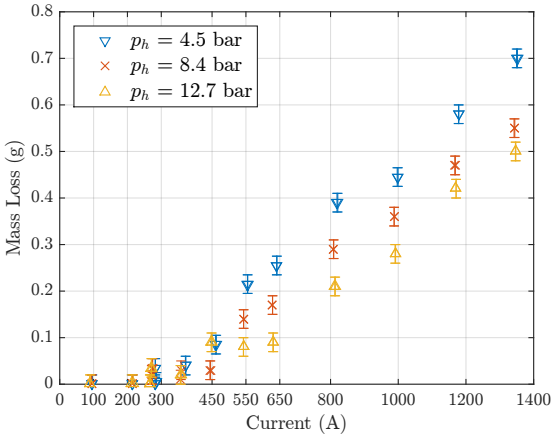

Figure 5. Ablated mass as a function of current. Initially all experiments with currents from 300 A to 1400 A used 10 ms of main current. Additional experiments with 300 A and below were performed, using longer periods of main current, but ablation was still too low to be measured accurately.

the CMM. This means the overestimation in the upstream section has to be higher than 10%. The data for the individual currents was only recorded with the scale and the scan, and indicates that the scanning method has an uncertainty around ±100 mg. Since the scale had an accuracy of ±20 mg, the values from weight measurements were used for figures 5 and 6. Figure 5 clearly shows that the mass loss due to ablation is increasing with current after a certain threshold around 350 A, and higher blow pressure reduced the amount of ablation for all currents.

A more general picture is obtained if the ablated mass is normalized to the total energy the arc dissipated during the high current phase, as shown in figure 6. This especially allows a comparison of tests with low current but long duration with tests of high current and short time. Experiments with 300 A for 40 ms are included, which had a similar specific ablation. Figure 6 shows even more clearly, that for the lower blow pressures the ablation increases sharply above a threshold current. Qualitatively this is similar to the results of Seeger [8]. Comparing the results quantitatively is not possible though, due to the different materials and gases.

5. Discussion

The scanning technique produced valuable results, even though the theoretical accuracy was not achieved. It was not possible to detect the edge of the contour on the scans with single-pixel resolution, since the edge is visible as a brightness gradient of roughly 20 px, or 100 µm. To improve the edge detection accuracy, painting the surface with different marker pens was considered, but all inks that were tried did not increase the detection accuracy by much. Other materials or changes to the background or lighting might be able to improve this technique. Additional to the edge detection uncertainty, the contour determined by the scan significantly overestimated the change of the radius around the throat compared with the CMM, as shown in figure 7. This is attributed to the fact that the gap where the two nozzle halves are joined is not perfectly gas-tight. The tests with 800 A and above showed erosion on the mating surface, up to to the sealing cord groove, which was likely caused by hot gas entering the gap. This erosion most probably eroded the contour edge as well, which means the assumption of cylindrical symmetry does not hold perfectly.

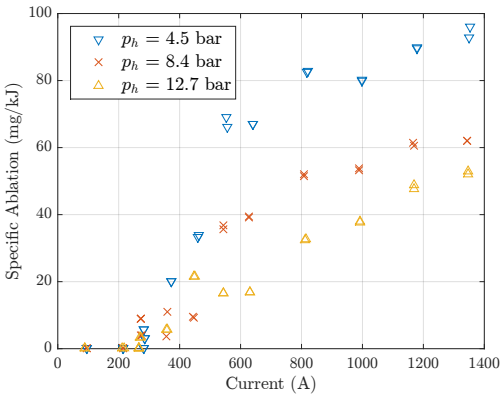

Figure 6. Ablated mass normalized to the energy dissipated by the arc during the main current phase, as function of current. Below 350 A, the ablation rate is about as low as the measuring inaccuracy, above that it rises with current.

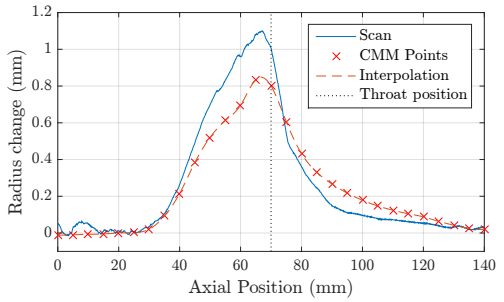

Figure 7. Total change of geometry (see fig 1) due to ablation. Determined by the flatbed scans and the coordinate measurement machine, after the entire measurement series for the 12.4 bar nozzle.

The results of the scans and the CMM (see fig. 7) both show the ablation as a function of axial position. Ablation starts at the position of the upstream contact (40 mm), increases towards the throat position (70 mm) and sharply decreases afterwards. In the diverging part of the nozzle, from 80 mm up to the downstream contact at 120 mm the amount of ablation is much smaller than in the upstream section. One possible reason for this could be higher arc power in the upstream section. Alternatively, the percentage of the dissipated energy arc that contributes to ablation compared with other cooling mechanisms is higher upstream. Higher blow pressures leads to higher arc power and lower ablation rate at the same time. This means, with increasing blow pressure the overall share of the ablation as cooling mechanism is reduced. However the present data does not allow for a quantification or explanation of this effect, since too many factors are still unknown. One of them is the combustion of PMMA with the oxygen of blowing air. According to [9], combustion of 1 g of PMMA yields a similar energy than what is required to vaporize it. This means, it is not possible to determine the energy balance of the ablation properly as long as air is used.

6. Conclusions

The methods described in section 3 worked with an accuracy as expected. Higher weighing accuracy is hard to achieve since it involves including effects like changes in PMMA density due to humidity, or changes in buoyancy due to changes in air pressure. The scanning method could probably be improved by enhancing the scan quality and the edge detection. The results shown in this paper agree well with previous findings [3], which indicate that increasing blow pressure is shifting the $u(i)$ curve towards more favourable conditions for passive oscillation breakers. Additionally it can be seen qualitatively that the threshold current above which ablation starts (300 A to 500 A according to figure 5) coincides with the point where the $u(i)$ changes to unfavorable (flat/rising) conditions (see fig. 4). If this is combined with the fact that the share of ablative cooling is increasing in the same region, the onset of significant ablation is directly correlated with the $u(i)$ curve getting flat.

Acknowledgements

The authors would like to thank ABB Switzerland for financial support, as well as E. Panousis of ABB CRC Switzerland for the frequent discussions.

References

[1] B. Bachmann et al. Development of a 500kV Airblast HVDC Circuit Breaker. *IEEE Trans. on Power Apparatus and Systems*, PAS-104(9):2460–2466, 1985. doi:10.1109/TPAS.1985.318991.

[2] T. Schultz et al. Circuit Breakers for Fault Current Interruption in HVDC Grids. In *VDE-Fachtagung Hochspannungstechnik*, 2016. doi:10.3929/ethz-a-010795297.

[3] M.M. Walter. *Switching Arcs in Passive Resonance HVDC Circuit Breakers*. PhD thesis, ETH Zürich, 2013. doi:10.3929/ethz-a-010112102.

[4] L. Muller. Modelling of an ablation controlled arc. *J Phys D: Appl Phys*, 26(8):1253–1259, 1993. doi:10.1088/0022-3727/26/8/015.

[5] L.S.J. Bort et al. Effects of nozzle and contact geometry on arc voltage in gas circuit-breakers. In *2016 IEEE Intern. Conf. on High Voltage Eng. and Appl.*, 2016. doi:10.1109/ICHVE.2016.7800700.

[6] A. Ritter et al. Five years of pulsed current testing for HVDC switchgear. In *2016 IEEE Intern. Conf. on High Voltage Eng. and Appl.*, 2016. doi:10.1109/ICHVE.2016.7800658.

[7] H. Schmid et al. Measuring a Small Number of Samples, and the 3v Fallacy: Shedding Light on Confidence and Error Intervals. *IEEE Solid-State Circuits Magazine*, 6(2):52–58, 2014. doi:10.1109/MSSC.2014.2313714.

[8] M. Seeger et al. Experimental study on PTFE ablation in high voltage circuit-breakers. *J Phys D: Appl Phys*, 39(23):5016–5024, 2006. doi:10.1088/0022-3727/39/23/018.

[9] B.T. Rhodes et al. Burning rate and flame heat flux for PMMA in a cone calorimeter. *Fire Safety Journal*, 26(3):221–240, 1996. doi:10.1016/S0379-7112(96)00025-2.